Implantation of Dedifferentiated Fat Cells Ameliorated ANCA Glomerulonephritis by Immunosuppression and Increases in TSG-6

Kei Utsunomiya
Nihon University School of Dentistry Graduate School of Dentistry at Matsudo
Takashi Maruyama
Nihon University School of Medicine Graduate School of Medicine
Satoshi Shimizu
Nihon University School of Medicine Graduate School of Medicine
Taro Matsumoto
Nihon University School of Dentistry Graduate School of Dentistry
Morito Endo
Hachinohe Gakuin University
Hiroki Kobayashi
Nihon University School of Medicine Graduate School of Medicine
Koichiro Kano
Nihon University College of Science and Technology Graduate School of Science and Technology
Masanori Abe
Nihon University School of Medicine Graduate School of Medicine
Noboru Fukuda (fukuda.noboru@nihon-u.ac.jp)
Nihon University

Research

Keywords: ANCA glomerulonephritis, Implantation, DFAT, TSG-6, Macrophage

Posted Date: October 5th, 2021

DOI: https://doi.org/10.21203/rs.3.rs-934207/v1

Abstract

We examined the effects of implantation of dedifferentiated fat (DFAT) cells on renal function, proteinuria and glomerulonephritis in SCG mice as a preclinical study of DFAT cell therapy for antineutrophil cytoplasmic antibody (ANCA) glomerulonephritis and investigated mechanisms underlying the immunosuppressive effects of the implantation of DFAT cells. After their intravenous infusion, almost all DFAT cells were trapped in the lung and not delivered into the kidney. Implantation of DFAT cells in SCG mice suppressed glomerular crescent formation, decreased urinary protein excretions, and increased expression of tumor necrosis factor-stimulated gene-6 (TSG-6) mRNA, protein and immunostaining in kidney from these mice. Implantation of DFAT cells increased the expression of microRNA 23b-3p in plasma, kidney and lung in SCG mice and decreased the expression of CD44 mRNA and increased the expression of prostaglandin E2 and interleukin-10 mRNAs in kidney from these mice. Implantation of DFAT cells increased expression of TSG-6 protein and decreased expression of tumor necrosis factor-a protein in kidney from SCG mice. Further, implantation of DFAT cells increased the expression of C-C motif chemokine ligand 17 protein, a chemokine for M2 macrophages, and decreased the expression of MCP-1 protein, a chemokine for M1 macrophages, in kidney from SCG mice. Survival rates were higher in SCG mice with implantation of DFAT cells than in SCG mice without implantation. These results indicate that implantation of DFAT cells suppressed renal injury including glomerular crescent formation in kidney from SCG mice while increasing the expression of TSG-6 without delivery of DFAT cells directly into kidney. Mechanisms underlying the effects of improvement of ANCA glomerulonephritis are associated with immunosuppressive effects by TSG-6 and the transition of M1 to M2 macrophages. These findings suggest that implantation of DFAT cells may become a cell therapy for ANCA glomerulonephritis.

Introduction

Implantation of mesenchymal stem cells (MSCs) has recently been reported to repair tissue injuries through anti-inflammatory and immunosuppressive effects [1, 2]. We established dedifferentiated fat (DFAT) cells that show identical characteristics to MSCs [3, 4]. Systematic infusion of MSCs has been reported to suppress graft rejection in animal models [5], and the implantation of MSCs has been investigated in clinical studies in which MSCs were reported to effectively inhibit graft-versus-host disease [6].

We have shown that DFAT cells have potential immunosuppressive effects. The systematic implantation of DFAT cells effectively ameliorated antibody-induced glomerulonephritis through immunosuppressive effects accompanied by the suppression of macrophage infiltration, and it increased the production of serum and renal tumor necrosis factor-stimulated gene-6 (TSG-6), which improved antibody-induced renal degeneration. These findings suggest that DFAT cells can potentially be a suitable cell source for the treatment of immunological progressive renal diseases [7]. Systematic implantation of DFAT cells effectively ameliorated monoclonal antibody (mAb) 1-22-3-induced glomerulonephritis through immunosuppressive effects accompanied by the suppression of macrophage infiltration and expression of interleukin (IL)-6, IL-10 and IL12β, and increased production of serum and renal TSG-6, which improved

the mAb 1-22-3-induced renal degeneration, through its immunosuppressive effects. Thus, DFAT cells may be a suitable cell source for the treatment of immunological progressive renal diseases.

Autoimmune-associated kidney diseases such as antineutrophil cytoplasmic antibody (ANCA) glomerulonephritis and lupus nephritis have been refractory diseases in the clinical field. ANCA glomerulonephritis is a nephropathy among the ANCA-associated vasculitides that commonly involve the glomerulus, including microscopic polyangiitis, granulomatosis with polyangiitis and eosinophilic granulomatosis [8]. ANCA is classified into a perinuclear pattern (P-ANCA) and cytoplasmic pattern (C-ANCA) by indirect immunofluorescence findings. The antigen for P-ANCA is mainly myeloperoxidase (MPO), which is almost positive in microscopic polyangiitis [9]. A typical renal pathological finding is that of glomerular necrotic crescent formation. Mild lesions of ANCA glomerulonephritis shows segmental necrotic glomerulonephritis, and almost sever lesion shows glomerular necrotic crescent formation [10].

The spontaneous crescentic glomerulonephritis-forming (SCG) mouse as a model for ANCA glomerulonephritis is a hybrid inbred strain established by brother-sister inbreeding of the BXSB mouse inducing crescent forming glomerulonephritis and the MRL/lpr mouse inducing ANCA-associated vasculitis. Thus, the SCG mouse is a genetic model mouse with the autoimmune promoting gene lpr [11]. The SCG mouse shows proteinuria and lymph node swelling, and crescent forming glomerulonephritis along with increases in MPO-ANCA and TNF-α from 8 weeks of age. In addition, SCG mice show systematic vasculitis of small vessels initially that gradually spreads to large vessels and each organ. Half of SCG mice show proteinuria by 90 days after birth, have an average survival period of around 120 days, and die from renal failure [12].

The number of patients with rapidly progressive glomerulonephritis has recently begun to rapidly increase in Japan as a cause of dialysis-introduced primary disease. ANCA glomerulonephritis is the most frequent disease leading to rapidly progressive glomerulonephritis and has a poor life prognosis because repeat relapses of this disease occur after transient improvement with steroid therapy [8].

In the present study, we examined the effects of the implantation of DFAT cells on renal function, proteinuria and glomerulonephritis in SCG mice as a preclinical study of DFAT cell therapy for ANCA glomerulonephritis and investigated mechanisms of the immunosuppressive effects of the implantation of DFAT cells.

Methods

Ethics and animals

This investigation conformed to the Guide for the Care and Use of Laboratory Animals published by the US National Institutes of Health (NIH Publication No. 85 – 23, 1996). The ethics committee of the Nihon University School of Medicine approved this study (approval no.: AP18MED021-1). Male SCG/Kj mice were purchased from the National Institutes of Biomedical Innovation, Health and Nutrition and were bred with female ICR mice (Charles River Laboratory Japan, Yokohama, Japan).

Preparation of DFAT cells from adipose tissue

Around 1 g of epididymal adipose tissue from six male ICR mice was treated with collagenase and centrifuged. Adipocytes were isolated from the top layer. More than 99% of the isolated cells were mature lipid-filled adipocytes. The mature adipocytes floating on top of the culture medium attached to the upper surface of the culture flasks within a few days. Approximately 10–20% of the adherent cells flattened out by day 3 and changed into a spindle-shaped morphology by day 7. The cells subsequently entered a proliferative log-phase upon inversion of the flasks and changing of the media and reached confluence by day 14. During this stage, the cells completely lose their lipid droplets and exhibit the fibroblast-like morphology of DFAT cells. Six different DFAT cells from six ICR mice, and combined them as allogenic DFAT cells.

Distribution of DFAT cells after implantation

DFAT cells from the ICR mice were labeled with PKH26 Red Fluorescent Cell Linker Kit for General Cell Membrane Labeling (Sigma Chemical, St. Louis, MO, USA). In total, 10^5 labeled DFAT cells were infused through the posterior orbital venous plexus of ICR mice. At 1 hour, 24 hours, and 1 week after the injection, kidney, aorta, liver and lungs were removed and fixed in 3% formalin in phosphate-buffered saline (PBS) and embedded in paraffin. Sections were observed under a fluorescence microscope (IX73, Olympus, Tokyo, Japan), and images were obtained with a digital imaging system.

Experimental protocols

Figure 2 shows the protocols used for the implantations of DFAT cells. ICR mice without implantation of DFAT cells were the control for SCG mice. SCG mice without implantation of DFAT cells were the control for the implantations of DFAT cells. Protocol 1 indicates SCG mice with single implantation of DFAT cells at 8 weeks of age. Protocol 2 indicates SCG mice with triple implantation of DFAT cells at 8, 9 and 10 weeks of age. Each mouse was sacrificed at 12 weeks of age, blood was sampled, and kidneys were removed. Protocol 3 indicates SCG mice with single implantation of DFAT cells at 8 weeks of age. Urine was collected from the mice at 12 to 17 weeks of age in metabolic cages, and urinary protein was determined with a Bio-Rad protein assay kit (Bio-Rad, Hercules, CA, USA). Serum blood urea nitrogen (BUN) and creatinine were measured by SRL, Inc. (Wako, Saitama, Japan). The MPO-ANCA titer was determined by an ELISA kit (MBL Laboratory, Tokyo, Japan).

Determination of renal injury

The 3-mm paraffin-embedded sections of removed renal cortex were stained with hematoxylin and eosin. Renal cortical thickness was measured under high magnification (×400). The glomerular injury score (GIS) was obtained by the following formula: $[(0 \times n0) + (1 \times n1) + (2 \times n2) + (3 \times n3) + (4 \times n4)]/50$. To semi-quantify the tubulointerstitial area, 20 areas of the renal cortex were randomly selected. The percentage of each area that showed sclerofibrotic change was estimated and assigned a score of 0, normal; 1, involvement of < 10% of the area; 2, involvement of 10–30% of the area; 3, involvement of >

30–50% of the area; or 4, involvement of > 50% of the area. The tubulointerstitial injury score (TIS) was similarly calculated as [(0 × n0) + (1 × n1) + (2 × n2) + (3 × n3) + (4 × n4)]/20.

Immunohistochemical analysis of TSG-6

For immunohistochemical analysis of TSG-6, rabbit polyclonal anti-TSG-6 antibody (Santa Cruz Biotechnology, Santa Cruz, CA, USA) diluted 1:500 was used as a first antibody and incubated for 30 min. Then, ImmPRESS Reagent (VECTOR LABORATORIES, Burlingame, CA, USA) was used as secondary antibodies. Counterstaining was then performed before the sections were examined under a light microscope.

RNA extraction and real-time PCR

Total RNA was extracted from renal medulla of kidney of 12-week-old mice with TRIzol reagent (Life Technologies) according to the manufacturer's instructions. Total RNA (1 μg) was reverse transcribed into cDNA with random 9-mers with an RNA PCR Kit (AMV) Ver. 3.0 (Takara Bio, Ohtsu, Japan). With the use of a StepOnePlus real-time PCR System (Applied Biosystems, USA), mRNA expression of TSG-6 (*Tnfaip6*), CD44 (*Cd44*), prostaglandin (PG) E2 (*Ptger2*), IL-10 (*Il10*), IL-1β (*Il1b*), tumor necrosis factor (TNF)-α (*Tnf*) and β-actin (*Actb*) as an internal control was determined by the SYBR Green method with Power UP SYBR® Green PCR Master Mix (Applied Biosystems, USA).

Amplifications were done at 95°C for 15 s, then 60°C for 60 s, and 95°C for 15 s with a GeneAmp PCR System 2700 (Applied Biosystems) for 55 cycles. After we determined the threshold cycle (Ct), we used the comparative Ct method to calculate the relative quantification of mRNA expression of the marker gene. The quality and concentration of the amplified PCR products were determined using an Agilent 2100 Bioanalyzer (Agilent, Palo Alto, CA, USA). Table 1 shows the sequences of these primers.

Quantification of miRNA

Peripheral blood was collected by cardiac blood samplings from three SCG mice each with or without implantation of DFAT cells and mixed with an equal volume of PBE buffer solution (containing 10% fetal bovine serum, 2 mM ethylenediaminetetraacetic acid and PBS. Peripheral blood mononuclear cells were isolated by the Percoll method. Kidneys and lungs from three SCG mice each with or without implantation of DFAT cells were homogenized and mixed in PBE buffer solution. Total RNA was isolated from the PBE-mixed samples from kidney and lung with TRIzol Reagent (Invitrogen, Waltham, MA, USA) according to the manufacturer's protocol. Total RNA was purified and ultimately eluted into 20 μL of RNase-free water. RNA quantity was assessed with a NanoDrop system (NanoDrop Products, Wilmington, DL, USA).

Sequencing libraries were constructed using the QIAseq™ miRNA Library Kit (Qiagen, Hilden, Germany) according to the manufacturer's protocols. The quality of the libraries was assessed with an Agilent Bioanalyzer using a High Sensitivity DNA chip (Agilent Technologies, Santa Clara, CA, USA). The pooled libraries of the samples were sequenced using NextSeq 500 (Illumina, Inc., San Diego, CA, USA) in 76-base pair single-end reads.

The QIAseq microRNA (miRNA) library kit adopts the Unique Molecular Indexes (UMI) system, enabling unbiased and accurate quantification of mature miRNAs. Original FASTQ files generated by NextSeq were uploaded to the Qiagen GeneGlobe Data Analysis Center (https://geneglobe.qiagen.com) and aligned to the miRBase v21 (http://www.mirbase.org) and piRNABank (http://pirnabank.ibab.ac.in/). All reads assigned to a particular miRNA or piRNA were counted, and the associated UMI were aggregated to count unique molecules. A matrix of the UMI counts of miRNA or piRNA was subjected to downstream analyses using StrandNGS 3.4 software (Agilent Technologies). The UMI counts were quantified using a Trimmed Mean of M-value method [13]. miRNAs were annotated against miRBase.

Western blot analysis

Renal medulla from mice were disrupted with lysis buffer (50 mM Tris·HCl, pH 8.0, 150 mM NaCl, 0.02% sodium azide, 100 μg/mL phenylmethylsulfonyl fluoride, 1 μg/mL aprotinin and 1% Triton X-100). Total proteins were extracted and purified with 100 μL of chloroform and 400 μL of methanol. Protein samples were boiled for 3 min and subjected to electrophoresis on 8% polyacrylamide gels and then transblotted to nitrocellulose membranes (Bio-Rad Laboratories). Blots were incubated with anti-TSG-6 polyclonal antibody (Santa Cruz Biotechnology), anti-TNF-α polyclonal antibody (Cell Signaling Technology, Danvers,MA, USA), anti-MCP-1 polyclonal antibody, (Biorbyt, Cambridge, UK), anti-TARC (C-C motif chemokine ligand 17 [CCL17]) polyclonal antibody (Invitrogen) and anti-beta actin antibody (Abcam, Cambridge, UK) in 5% non-fat milk in TBST solution (10 mM Tris·HCl, pH 8.0, 150 mM NaCl and 0.05% Tween 20) for 3 h at room temperature. The membrane was incubated with horseradish peroxidase-labeled secondary antibody (Sigma-Aldrich, St. Louis, MO, USA) for 1 h at room temperature and then washed with TBST once for 15 min and then four more times for 5 min each. Immune complexes on the membrane were detected by the enhanced chemiluminescence method (Amersham Pharmacia Biotech, Little Chalfont, Buckinghamshire, UK). Obtained bands were quantified by ImageStudio Lite (https://www.licor.com/bio/image-studio-lite).

Determination of regulatory T cell population

Spleen was removed and homogenized 4 weeks after implantation of 10^6 DFAT cells in SCG mice. Cells from spleen were labelled with fluorogenic antibodies CD4-APC-Cy7, CD25-AlexaFluor® 647 and FOXP3-PerCP5.5 to evaluate the proportion of $CD4^+$ $CD25^+$ $FOXP3^+$ regulatory T cells. Cells were fixed and permeabilized with a FOXP3 Staining Buffer Set according to the manufacturer's instructions and included the blocking step with 2% rat serum. Flow cytometry was performed with a FACSAria system, and data were analyzed using FlowJo 7.6.5 software.

Statistics

Values are reported as the mean ± SEM. Two-way ANOVA with the Bonferroni/Dunn procedure as a post-test was also used. A value of $P < 0.05$ was considered to be statistically significant.

Results

Distribution of implanted DFAT cells

In total, 10^5 PKH26-labeled DFAT cells were infused through the posterior orbital venous plexus in ICR mice. One hour after injection, these DFAT cells were trapped in the lung (Fig. 1) and were not delivered into the kidney, aorta, or liver. The PKH26-positive cells were trapped for one day and had disappeared from the lung by 1 week after implantation (data not shown).

Comparison of effects of single and triple implantations of DFAT cells on renal function, MPO-ANCA and TSG-6

We examined the effects of single and triple implantations of DFAT cells on renal function, plasma MPO-ANCA titer and expression of TSG-6 mRNA in kidney. Single and triple implantations of DFAT cells did not affect increased serum creatinine levels in SCG mice (Fig. 3A). Single implantations of DFAT cells significantly ($P < 0.05$) suppressed increased BUN levels in SCG mice, but triple implantations of DFAT cells had no significant effect on BUN levels (Fig. 3B). Single implantation of DFAT cells significantly ($P < 0.05$) suppressed increased plasma MPO-ANCA titer in SCG mice, whereas triple implantations of DFAT cells did not affect the plasma titer (Fig. 3C). Figure 3D shows the effects of single and triple implantations of DFAT cells on the expression of TSG-6 mRNA in kidney from SCG mice. Single implantations of DFAT cells significantly ($P < 0.05$) increased the amount of TSG-6 mRNA in kidney from SCG mice, whereas triple implantations of DFAT cells had no significant effect on TSG-6 mRNA expression. Thus, the single implantations of DFAT cells rather effectively improved renal function, decreased the MPO-ANCA titer, and increased the expression of TSG-6 in kidney in SCG mice compared with the effects from triple implantations of DFAT cells. Therefore, we examined single implantations of DFAT cells in SCG mice in the following experiments.

Effects of implantation of DFAT cells on renal injury in SCG mice

The glomerulus from 12-week-old SCG mice showed cellular crescent formation (arrowheads in Fig. 4A). Implantation of DFAT cells suppressed glomerular cellular crescent formation. The GIS and TIS were significantly ($P < 0.05$) higher in kidney from SCG mice than those from ICR mice. Implantation of DFAT cells did not significantly affect the increased GIS and TIS in SCG mice (Figs. 4B, C).

Effects of implantation of DFAT cells on urinary protein excretion in SCG mice

Figure 5 shows the effects of implantation of DFAT cells on urinary protein excretion in SCG mice. After a single implantation of 10^5 DFAT cells in 13-week-old SCG mice, urinary protein excretion was significantly ($P < 0.05$) lower at 14, 15 and 16 weeks of age.

Expression of TSG-6 in kidney from SCG mice after implantation of DFAT cells

Figure 6 shows immunostaining of TSG-6 in SCG mice without and with implantation of DFAT cells. TSG-6 was positively stained in the glomerular mesangium but not in the nephrotubulus. After implantation of DFAT cells, immunostaining of TSG-6 was obviously increased as shown by the positive staining in the glomerular mesangium and nephrotubulus of kidney from SCG mice.

Expression of miRNA in plasma, kidney and lung

Effects of implantation of DFAT cells on expression of immune regulator mRNAs in kidney from SCG mice

Implantation of DFAT cells significantly ($P < 0.05$) decreased the abundance of CD44 mRNA (Fig. 7A) and significantly ($P < 0.05$) increased that of PGE2 mRNA (Fig. 7B) in kidney from SCG mice. Implantation of DFAT cells increased the abundance of IL-10 mRNA but not statistically significantly (Fig. 7C). Implantation of DFAT cells did not affect the abundance of IL1-β (Fig. 7D) or TNF-α (Fig. 7E) mRNA in kidney from SCG mice.

Effects of implantation of DFAT cells on expression of immune regulator proteins in kidney from SCG mice

Implantation of DFAT cells significantly ($P < 0.05$) increased the amount of TSG-6 protein in kidney from SCG mice (Fig. 8A), whereas it significantly ($P < 0.05$) decreased the amount of TNF-α protein in kidney from SCG mice (Fig. 8B). Implantation of DFAT cells significantly ($P < 0.05$) increased the amount of CCL-17 protein, a chemokine for M2 macrophage, in kidney from SCG mice (Fig. 9A), but it significantly ($P < 0.05$) decreased the amount of MCP-1 protein, a chemokine for M1 macrophage, in kidney from these mice (Fig. 9B).

Effects of implantation of DFAT cells on survival rate of SCG

Supplemental Fig. 1 shows the survival rates in SCG mice with and without implantation of DFAT cells. Seven weeks after the implantation of DFAT cells, the survival rate was 89% in SCG mice, whereas it was 67% in SCG mice without the implantation of DFAT cells.

Effects of implantation of DFAT cells on regulatory T-cell population in SCG mice

Figure 10 shows flow cytometric analyses used to evaluate the proportion of $CD4^+$ $CD25^+$ $FOXP3^+$ regulatory T cells in spleen from SCG mice with or without implantation of DFAT cells. There was no significant difference in the analyses between SCG mice with or without implantation of DFAT cells.

Discussion

In the present experiments, we first evaluated delivery of DFAT cells intravenously infused in SCG mice. Almost all of the DFAT cells were trapped in the lung and did not reach the kidney. Despite the non-delivery of DFAT cells into the kidney, the implantation of DFAT cells improved renal function (decrease in BUN), suppressed the expression of inflammatory cytokine MCP-1, and decreased urinary excretion of protein in SCG mice. We also previously showed that DFAT cells intravenously infused were trapped mainly in the lungs without reaching the kidneys, and implantation of DFAT cells reduced proteinuria and improved glomerulosclerosis and interstitial fibrosis in mAb 1-22-3-induced glomerulonephritis in rats. Moreover, the systematic implantation of DFAT cells through the vein was more effective in improving mAb 1-22-3-induced glomerulonephritis than direct implantation of DFAT cells through the renal artery [7]. Thus, it is surmised that the DFAT cells trapped in lungs released substrates that may have then reached the kidney to improve ANCA glomerulonephritis in the SCG mice. Mechanisms underlying the immunosuppressive effects of the MSCs trapped in the lungs after intravenous implantation have been reported to be associated with exosomes including cytokines, miRNAs and peptides that improve acute graft-versus-host disease and immune-induced acute kidney injury [14, 15]. In terms of the mechanisms underlying the induction of immunosuppressive and anti-inflammatory effects by lung-trapped MSCs and DFAT cells, these effects of the implantation of MSCs are associated with the secretion of soluble factors with paracrine actions that are mediated by exosomes. Exosomes are predominantly released from the endosomal compartment and contain miRNA, cytokines, and proteins from MSCs. Recent studies in animal models suggest that exosomes have significant potential as a novel alternative to whole-cell therapies [16]. Bruno et al. [14] showed that exosomes derived from MSCs improve acute tubular injury. Chaubey et al. [17] reported that implantation of MSCs improved experimental bronchopulmonary dysplasia in part via exosome-associated factor TSG-6. Thus, DFAT cell-derived exosomes may improve ANCA glomerulonephritis by increasing TSG-6 in kidney. It is thought that the direct infusion of exosomes from ex vivo-cultured DFAT cells will be effective immunosuppressive therapy for ANCA glomerulonephritis.

In the present experiments, the single implantation of DFAT cells was rather more effective in improving renal function, decreasing MPO-ANCA titer, and increasing the expression of TSG-6 in the kidney of SCG mice than the triple implantations of DFAT cells. Recently, single implantation has been also reported to show rather effective immunosuppressive effects on autoimmune-induced colitis in mice [19] and osteoarthritis in a clinical study [20]. Thus, the single implantation of DFAT cells effectively induced the immunosuppression of ANCA glomerulonephritis, which may be associated with exosome release from the lungs.

We confirmed the ANCA glomerulonephritis as cellular crescent formation in kidney from the 12-week-old SCG mice. Neumann et al. [20] showed that the number of glomerular crescent formations increased along with aging. In addition, plasma levels of MPO-ANCA concentrations in SCG mice were higher than those in ICR mice. Implantation of DFAT cells decreased the GIS but did not affect the TIS of kidney from

ICR mice. These results indicate that implantation of DFAT cells mainly improved the glomerular injury whereas their implantation did not appreciably affect nephrotubular degeneration.

Concerning the immunosuppressive effects of MSCs, two mechanisms have been considered to regulate immunoactivity [21]. One mechanism has been reported in which MCSs release TSG-6 that suppresses adhesion molecule CD44 on T cells to inhibit T-cell activity and cell infiltrations, by which the regulatory T cells are increased to obtain immune tolerance [22]. In the other reported mechanism, MSCs release PGE2 that induces the transition of M1 to M2 macrophages [24].

In our previous study, we observed that the systematic implantation of DFAT cells effectively ameliorated mAb 1-22-3-induced glomerulonephritis through immunosuppressive effects accompanied by the suppression of macrophage infiltration and expression of IL-6, IL-10 and IL-12β, and increased the production of serum and renal TSG-6, which improved the mAb 1-22-3-induced renal degeneration through the immunosuppressive effects of TSG-6 [7].

In the present experiments, the implantation of DFAT cells markedly increased the expression of TSG-6 mRNA and proteins in kidney from SCG mice, even though no DFAT cells were delivered into the kidney. The implantation of DFAT cells did not affect the number of regulatory T cells in spleen from SCG mice. However, implantation of DFAT cells decreased the expression of CD44 mRNA in kidney from these mice, thus suggesting that DFAT cells may regulate immunoactivity by suppression of the activity and invasion of T cells.

Moreover, expression of PGE2 and IL-10 mRNAs in the present experiments was increased in kidney from SCG mice after the implantation of DFAT cells. After the implantation of DFAT cells, the expression of MCP-1 as M1 macrophage chemokines was decreased in kidney of SCG mice, and that of CCL17 as a chemokine for M2 macrophages was increased in kidney of SCG mice. These results indicate that mechanisms underlying the immunoregulatory effects of DFAT cells appear to be associated with induction of the transition of M1 to M2 macrophages with production of inflammatory cytokine IL-10.

Because the implantation of DFAT cells may improve ANCA glomerulonephritis through increases in TSG-6 in kidney, which may be mediated by exosomes, we analyzed the expression of miRNAs in plasma, kidney and lungs in SCG mice after the implantation of DFAT cells. Expression of miR23b-3p was obviously higher in plasma, kidney and lung from these mice with implantation of DFAT cells compared to those in plasma, kidney and lung from SCG mice without implantation of DFAT cells. These results indicate that the increases in TSG-6 in kidney from SCG mice may be mediated by miR23b-3p delivered by the exosomes.

In the present experiments, the survival rate was higher in SCG mice with rather than without the implantation of DFAT cells. Longer-term investigations of the survival rate and side effects such as tumor genesis are needed for application of the implantation of DFAT cells for ANCA glomerulonephritis as the average survival period of SCG mice is only 120 days.

Conclusions

In conclusion, the intravenous implantation of DFAT cells in SCG mice suppressed renal injury including glomerular cellular crescent formation in kidney and increased the expression of TSG-6 without the delivery of DFAT cells directly into kidney. Mechanisms underlying the improvement of ANCA glomerulonephritis are associated with the immunosuppressive effects of TSG-6 and the transition of M1 to M2 macrophages. These findings suggest that implantation of DFAT cells can be a potential cell therapy for ANCA glomerulonephritis.

Abbreviations

ANCA: antineutrophil cytoplasmic antibody; BUN: blood urea nitrogen; CCL17: C-C motif chemokine ligand 17; DFAT: dedifferentiated fat; GIS: glomerular injury score; IL: interleukin; mAb: monoclonal antibody; miRNA: microRNA; MSCs: mesenchymal stem cells; PBS: phosphate-buffered saline; TIS: tubulointerstitial injury score; TNF: tumor necrosis factor; TSG-6: tumor necrosis factor-stimulated gene-6; UMI: Unique Molecular Indexes.

Declarations

Acknowledgements

We thank Miyuki Fukazawa for technical support.

Authors' contributions

KU and SS contributed to the practical experiments in rats and data collection. TM (Takashi Maruyama) and NF were involved in the conception and design of the study, manuscript writing, and data analysis and interpretation. TM (Tarao Matsumoto) and KK contributed to preparation of DFAT cells. ME contributed to morphological analysis. KU, SS, NF, TM (Takashi Maruyama), HK and MA contributed to data analysis and interpretation. All authors read and approved the final manuscript.

Funding

This study was supported in animal collections, preparing reagents and analysis of data by a Grant-in-Aid for Scientific Research from MEXT 2018-2020 (18K08255) and Nihon University Multidisciplinary Research Grant for 2020.

Availability of data and materials

The data that support the findings of this study are available from the corresponding author upon reasonable request.

Ethics approval and consent to participate

This investigation conformed to the Guide for the Care and Use of Laboratory Animals published by the US National Institutes of Health (NIH Publication No. 85-23, 1996). The ethics committee of the Nihon University School of Medicine approved

this study (approval no.: AP18MED021-1).

Consent of publication

There is no identifiable information from all participants.

References

1. Ortiz LA, Gambelli F, McBride C, Gaupp D, Baddoo M, Kaminski N, et al. Mesenchymal stem cell engraftment in lung is enhanced in response to bleomycin exposure and ameliorates its fibrotic effects. Proc Natl Acad Sci USA. 2003;100:8407–11.
2. Kanazawa H, Fujimoto Y, Teratani T, Iwasaki J, Kasahara N, Negishi K, et al. Bone marrow-derived mesenchymal stem cells ameliorate hepatic ischemia reperfusion injury in a rat model. PLoS One. 2011;6:e19195.
3. Yagi K, Kondo D, Okazaki Y, Kano K. A novel preadipocyte cell line established from mouse adult mature adipocytes. Biochem Biophys Res Commun. 2004;321:967–74.
4. Matsumoto T, Kano K, Kondo D, Fukuda N, Iribe Y, Tanaka N, et al. Mature adipocyte-derived dedifferentiated fat cells exhibit multilineage potential. J Cell Physiol. 2008;215:210–22.
5. Uccelli A, Moretta L, Pistoia V. Mesenchymal stem cells in health and disease. Nat Rev Immunol. 2008;28:726–36.
6. Kuzmina LA, Petinati NA, Parovichnikova EN, Lubimova LS, Gribanova EO, Gaponova TV, et al. Multipotent mesenchymal stromal cells for the prophylaxis of acute graft-versus-host disease-a phase II study. Stem Cells Int. 2012;2012:968213.
7. Maruyama T, Fukuda N, Matsumoto T, Kano K, Endo M, Kazama M, et al. Systematic implantation of dedifferentiated fat cells ameliorated monoclonal antibody 1-22-3-induced glomerulonephritis by immunosuppression with increases in TNF-stimulated gene 6. Stem Cell Res Ther. 2015;6:80.
8. Jennette JC, Falk RJ, Bacon PA, Basu N, Cid MC, Ferrario F, et al. 2012 revised International Chapel Hill Consensus Conference Nomenclature of Vasculitides. Arthritis Rheum. 2013;65:1–11.
9. Kitching AR, Anders HJ, Basu N, Brouwer E, Gordon J, Jayne DR, et al. ANCA-associated vasculitis. Nat Rev Dis Primers. 2020;6:71.
10. Jennette JC, Nachman PH. ANCA glomerulonephritis and vasculitis. Clin J Am Soc Nephrol. 2017;12:1680–91.
11. Kinjoh K, Kyogoku M, Good RA. Genetic selection for crescent formation yields mouse strain with rapidly progressive glomerulonephritis and small vessel vasculitis. Proc Natl Acad Sci USA. 1993;90:3413–7.

12. Ishida-Okawara A, Ito-Ihara T, Muso E, Ono T, Saiga K, Nemoto K, et al. Neutrophil contribution to the crescentic glomerulonephritis in SCG/Kj mice. Nephrol Dial Transplant. 2004;19:1708–15.
13. Robinson MD, Oshlack A. A scaling normalization method for differential expression analysis of RNA-seq data. Genome Biol. 2010;11:R25.
14. Bruno S, Grange C, Deregibus MC, Calogero RA, Saviozzi S, Collino F, et al. Mesenchymal stem cell-derived microvesicles protect against acute tubular injury. J Am Soc Nephrol. 2009;20:1053–67.
15. Tsuji K, Kitamura S, Wada J. Secretomes from mesenchymal stem cells against acute kidney injury. Stem Cell Int. 2018;8693137:1–14.
16. Rani S, Ryan AE, Griffin MD, Ritter T. Mesenchymal stem cell-derived extracellular vesicles: Toward cell-free therapeutic applications. Mol Ther. 2015;23(5):812–23.
17. Chaubey S, Thueson S, Ponnalagu D, Alam MA, Gheorghe CP, Aghai Z, et al. Early gestational mesenchymal stem cell secretome attenuates experimental bronchopulmonary dysplasia in part via exosome-associated factor TSG-6. Stem Cell Res Ther. 2018;9(1):173.
18. Chang YL, Lo HY, Cheng SP, Chang KT, Lin XF, Lee SP, et al. Therapeutic effects of a single injection of human umbilical mesenchymal stem cells on acute and chronic colitis in mice. Sci Rep. 2019;9(1):5832.
19. Magri C, Schramme M, Febre M, Cauvin E, Labadie F, Saulnier N, et al. Comparison of efficacy and safety of single versus repeated intra-articular injection of allogeneic neonatal mesenchymal stem cells for treatment of osteoarthritis of the metacarpophalangeal/metatarsophalangeal joint in horses: a clinical pilot study. PLoS One. 2019;14(8):e0221317.
20. Neumann I, Birck R, Newman M, Schnülle P, Kriz W, Nemoto K, et al. SCG/Kinjoh mice: a model of ANCA-associated crescentic glomerulonephritis with immune deposits. Kidney Int. 2003;64:140–8.
21. Prockop DJ. Concise review: Two negative feedback loops place mesenchymal stem/stromal cells at the center of early regulators of inflammation. Stem Cells. 2013;31:2042–6.
22. Kato T, Okumi M, Tanemura M, Yazawa K, Kakuta Y, Yamanaka K, et al. Adipose tissue-derived stem cells suppress acute cellular rejection by TSG-6 and CD44 interaction in rat kidney transplantation. Transplantation. 2014;98:277–84.
23. Furuhashi K, Tsuboi N, Shimizu A, Katsuno T, Kim H, Saka Y, et al. Serum-starved adipose-derived stromal cells ameliorate crescentic GN by promoting immunoregulatory macrophages. J Am Soc Nephrol. 2013;24:587–603.

Tables

Table1

Sequences of primers for real-time PCR

Tnfaip6	Forward 5’ to 3’	GCT GTC CTG GAA CTC ACT TTG
	Reverse 5’ to 3’	GAG GCA GGT GGA TTT CTG AG
Cd44	Forward 5’ to 3’	TCC TTC TTT ATC CGG AGC AC
	Reverse 5’ to 3’	CCT GGA GTC CTT GGA TGA GT
Ptger2	Forward 5’ to 3’	ATC ACC TTC GCC ATA TGC TC
	Reverse 5’ to 3’	GCT CGG AGG TCC CAC TTT
Tnf	Forward 5’ to 3’	TCT TCT CAT TCC TGC TTG TGG
	Reverse 5’ to 3’	GGT CTG GGC CAT AGA ACT GA
Il10	Forward 5’ to 3’	CAG AGC TCC TAA GAG AGT TGT GAA
	Reverse 5’ to 3’	TCA TCA AAG GAT CTC CCT GGT
Il1b	Forward 5’ to 3’	AGT TGA CGG ACC AAA G
	Reverse 5’ to 3’	AGC TGG ATG CTC TCA TCA GG
Actb	Forward 5’ to 3’	CCA ACC GTG AAA AGA TGA CC
	Reverse 5’ to 3’	ACC AGA GGC ATA CAG GGA CA

Table 2

Exressions of micro RNA in plasma, kidney and lung in SCG with or without implantation of DFAT cells

miRNA	SCG plasma	SCG plasma + DFAT	SCG kidney	SCG kidney + DFAT	SCG lung	SCG lung + DFAT
miR214-5p	2	10	202	153	210	269
miR1247-3p	27	80	20	17	18	12
miR326-5p	0	0	5	10	10	7
miR204-3p	5	7.5	44	41	14	13
miR23b-3p	643	1203.5	47281	54550	79636	98642

Figures

Figure 1

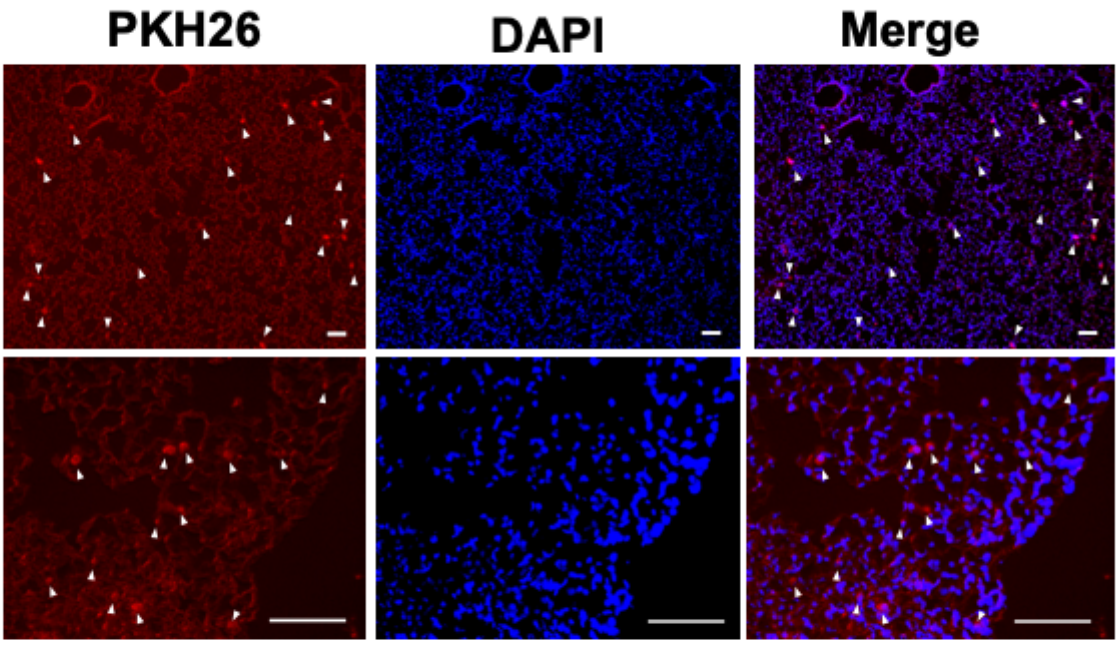

Figure 1

Distribution of implanted DFAT cells. In total, 105 of PKH26-labeled DFAT cells were infused through the posterior orbital venous plexus in ICR mice. One hour, 24 hours, and one week after the injection, kidney, aorta, liver and lungs were removed and fixed in 3% formalin in PBS and embedded in paraffin. Arrowheads indicate trapped DFAT cells. Bar = 50 μm. DFAT dedifferentiated fat

Figure 2

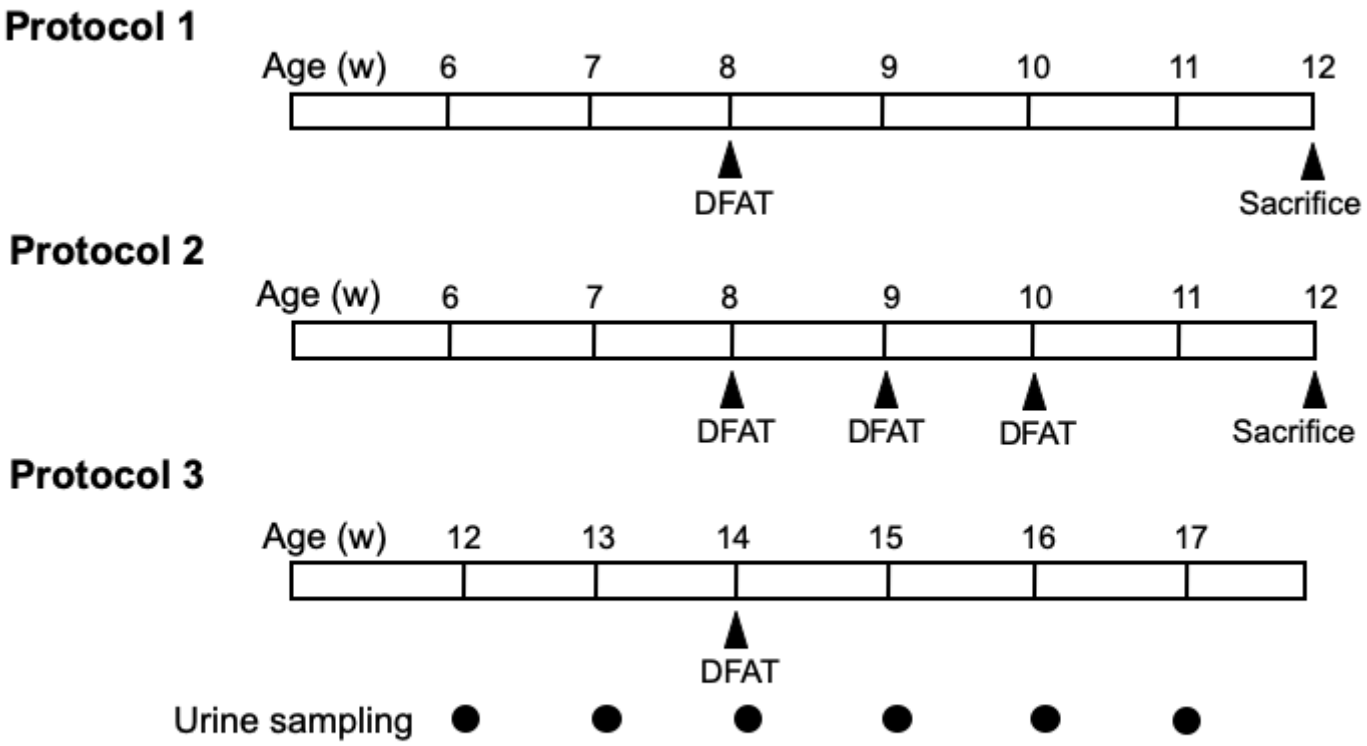

Figure 2

Experimental protocols for the implantations of DFAT cells in SCG mice. Protocol 1: SCG mice with single implantation of DFAT cells at 8 weeks of age. Protocol 2: SCG mice with triple implantation of DFAT cells at 8, 9 and 10 weeks of age. Each mouse was sacrificed at 12 weeks of age, its blood sampled, and its kidney removed. Protocol 3: Excreted urinary protein was collected from SCG mice at 12 to 17 weeks of age in metabolic cages. DFAT dedifferentiated fat

Figure 3

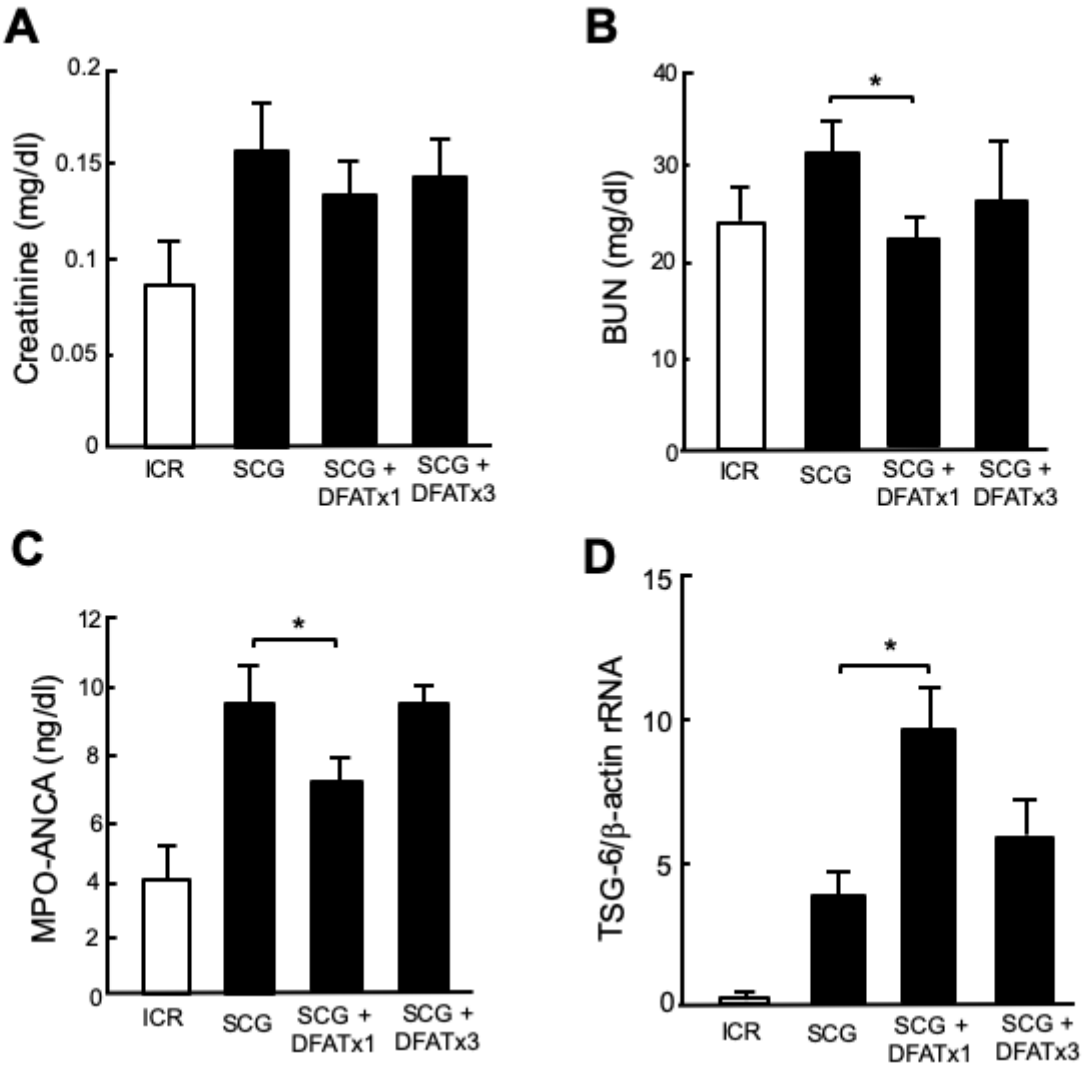

Figure 3

Comparison of single and triple implantations of DFAT cells for renal function, MPO-ANCA titer and expression of TSG-6 mRNA in kidney from SCG mice. SCG mice were infused with 105 of DFAT cells through the posterior orbital venous plexus once at 8 weeks of age (DFAT ×1) or three times at 8, 9 and 10 weeks of age (DFAT ×3). Each mouse was sacrificed at 12 weeks of age, its blood sampled, and its kidney removed . Total RNA was extracted from renal cortex and medulla from kidney, and mRNA expression of TSG-6 was determined by a real-time PCR system. Data are shown as the mean ± SEM (n = 4). *P < 0.05 in the indicated columns. BUN blood urea nitrogen; MPO-ANCA myeloperoxidase-antineutrophil cytoplasmic antibody; SEM standard error of the mean; TSG-6 tumor necrosis factor-stimulated gene-6

Figure 4

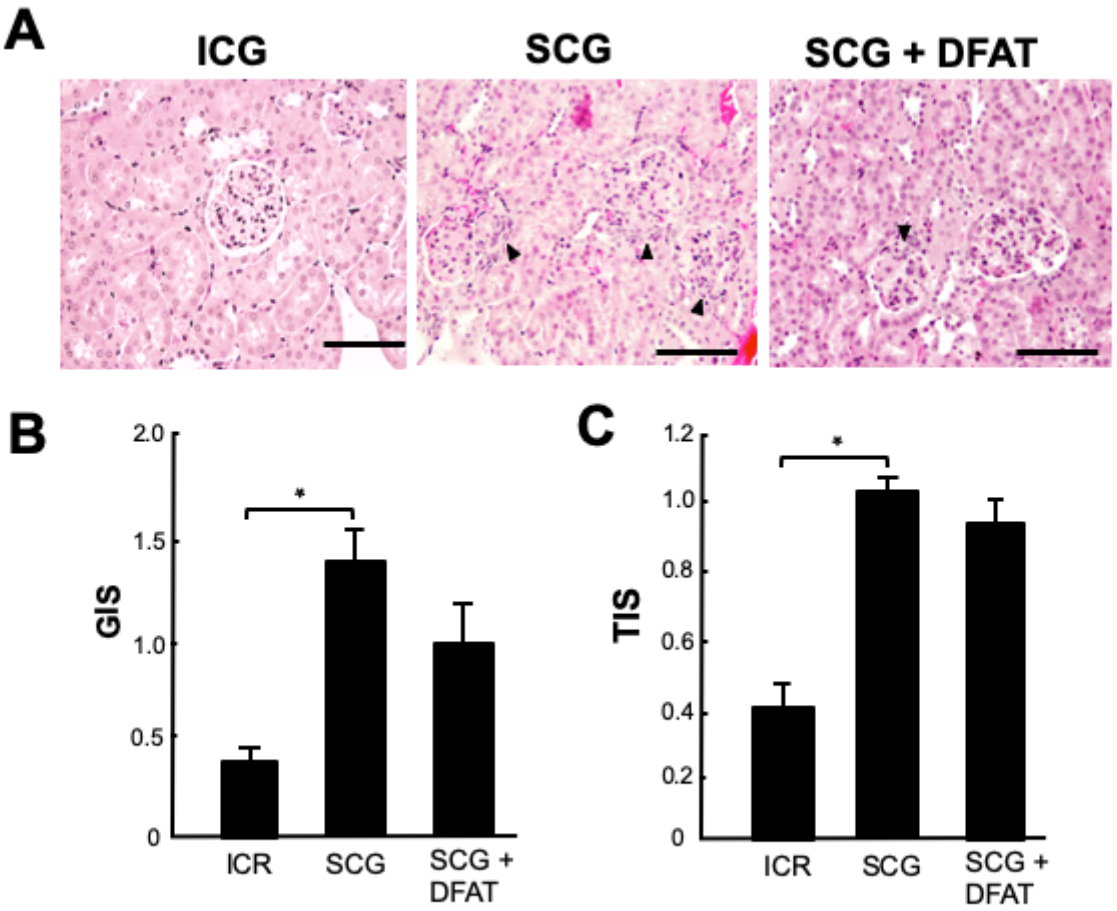

Figure 4

Effects of implantation of DFAT cells on renal injury in SCG mice. SCG mice were infused with 105 DFAT cells through the posterior orbital venous plexus once at 8 weeks of age. Mice were sacrificed at 12 weeks of age, and their kidneys were removed. (A) The paraffin-imbedded sections of the removed renal cortex were stained with hematoxylin and eosin. Arrowheads indicate cellular crescent formation in the glomerulus. (B) Glomerular injury score (GIS). (C) Tubulointerstitial injury score (TIS). Data are the mean ± SEM (n = 6). *P < 0.05 in the indicated columns. Bar = 50 μm. DFAT dedifferentiated fat; SEM standard error of the mean

Figure 5

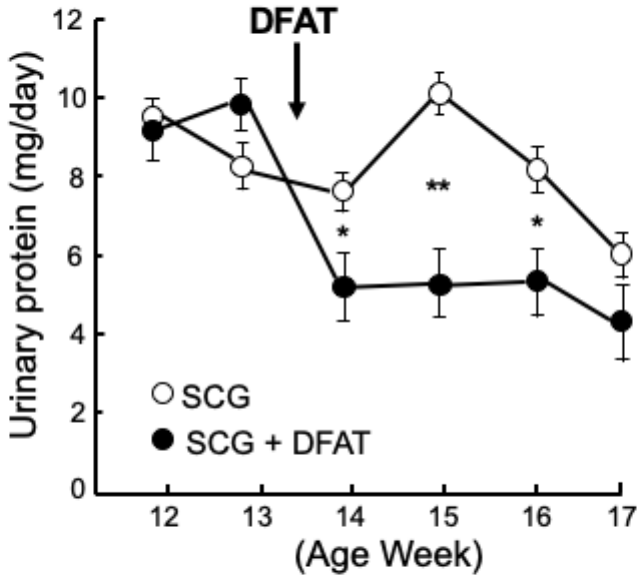

Figure 5

Effects of implantation of DFAT cells on urinary protein excretion in SCG mice. SCG mice were infused with 105 DFAT cells through the posterior orbital venous plexus once at 8 weeks of age. Excreted urinary protein was collected from the mice at 12 to 17 weeks of age in metabolic cages. Data are the mean ± SEM (n = 6). *P < 0.05 and **P < 0.01 between with and without implantation of DFAT cells. DFAT dedifferentiated fat; SEM standard error of the mean

Figure 6

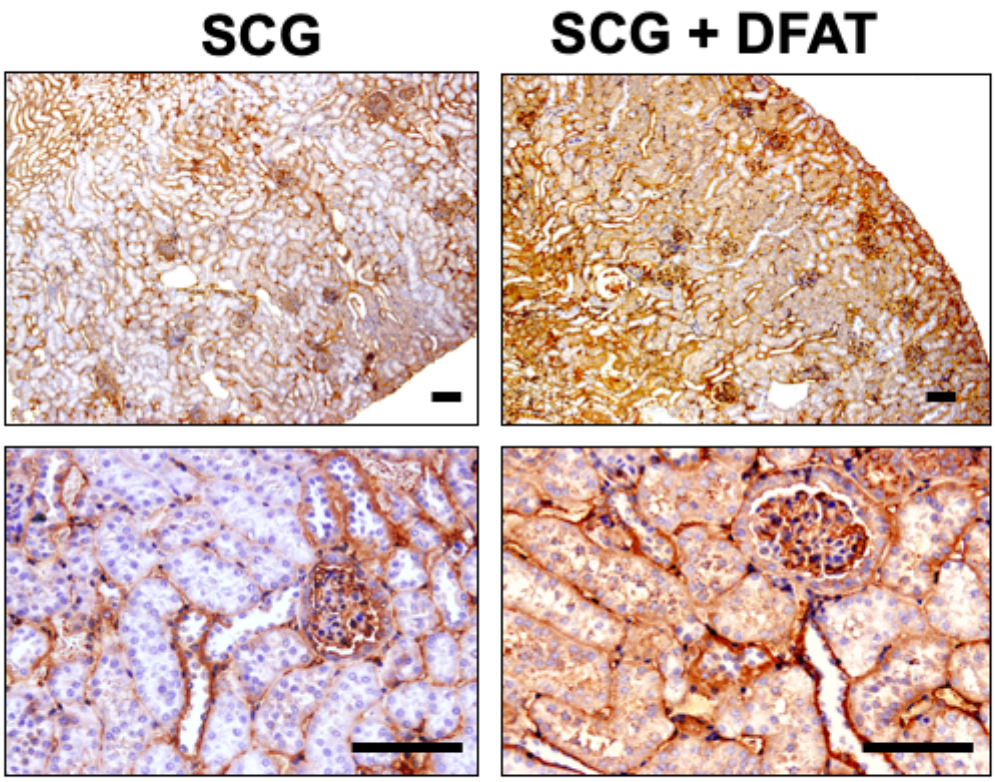

Figure 6

Expression of TSG-6 in kidney from SCG mice after implantation of DFAT cells. SCG mice were infused with 105 DFAT cells through the posterior orbital venous plexus once at 8 weeks of age. Mice were sacrificed at 12 weeks of age, and kidneys were removed. The 3-mm paraffin sections of the removed renal cortex were stained with rabbit polyclonal anti-TSG-6 antibody. Bar = 50 μm. DFAT dedifferentiated fat; TSG-6 tumor necrosis factor-stimulated gene-6

Figure 7

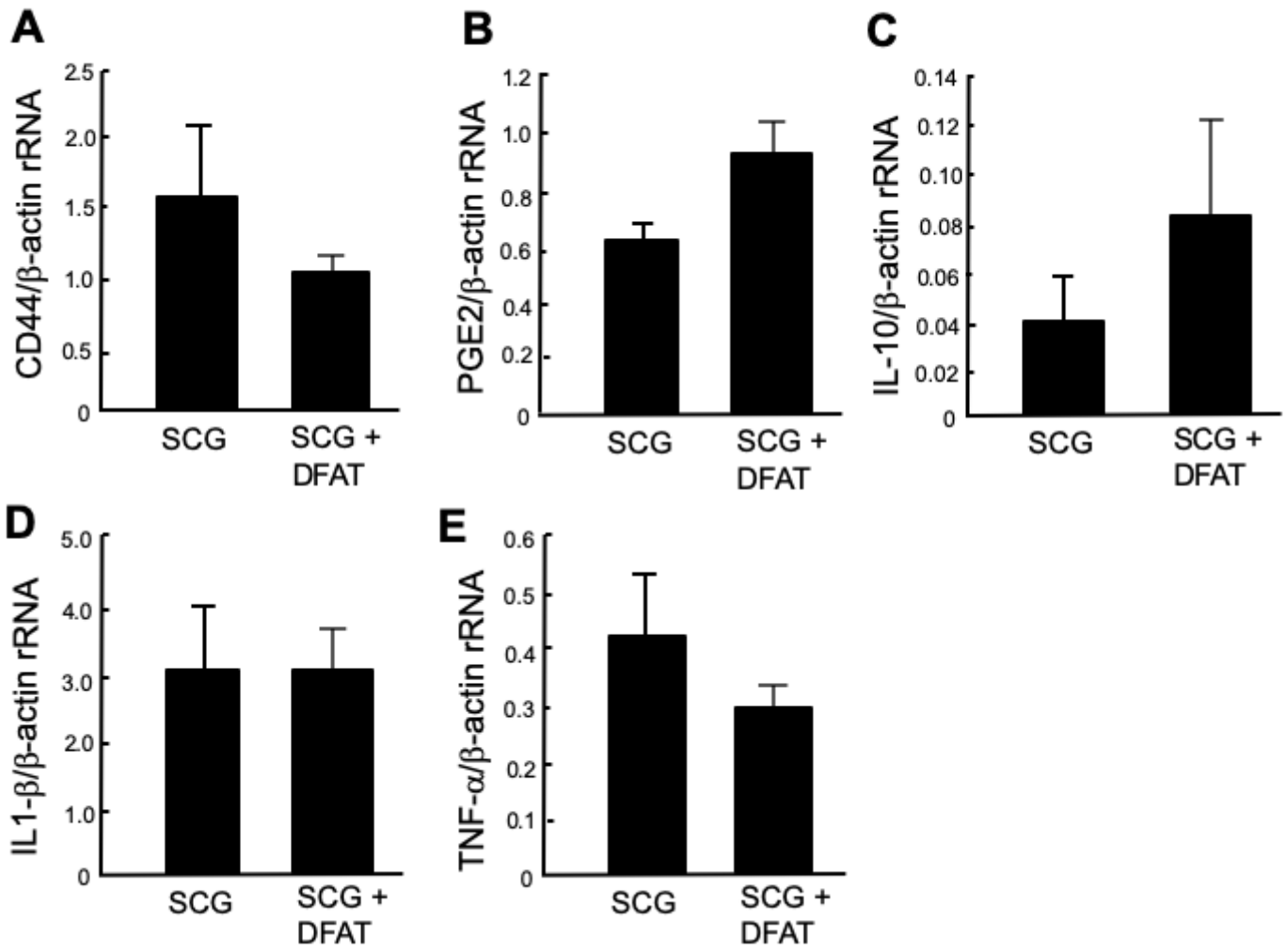

Figure 7

Effects of implantation of DFAT cells on the expression of immune regulator mRNAs in kidney from SCG mice. SCG mice were infused with 105 DFAT cells through the posterior orbital venous plexus once at 8 weeks of age. Mice were sacrificed at 12 weeks of age, and kidneys were removed. Total RNA was extracted from the renal medulla of kidneys with TRIzol reagent. PGE2, IL-10, IL-1β, TNF-α and β-actin as an internal control were determined by SYBR Green method. Data are the mean ± SEM (n = 4). DFAT dedifferentiated fat; IL interleukin; PGE2 prostaglandin E2, TNF, tumor necrosis factor

Figure 8

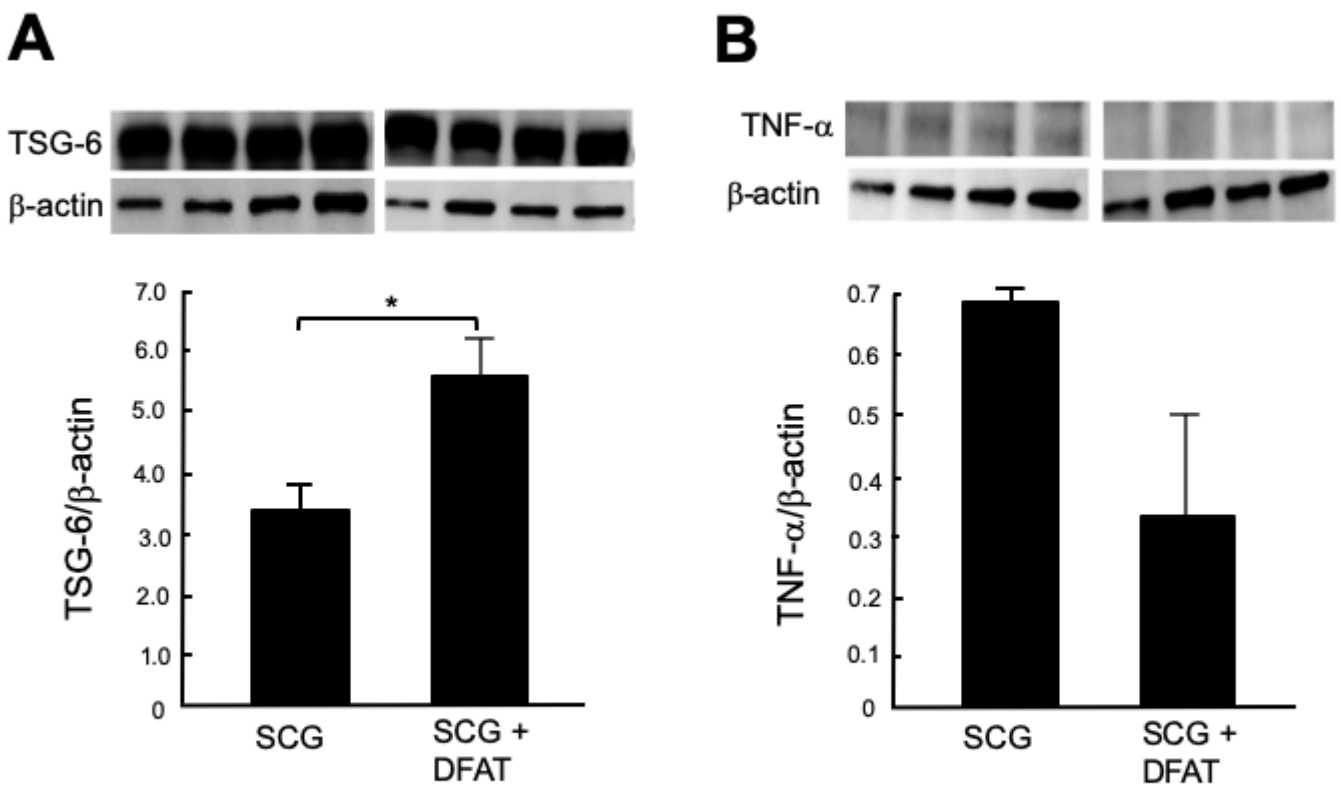

Figure 8

Effects of implantation of DFAT cells on expression of TSG-6 and TNF-α proteins in kidney from SCG mice. SCG mice were infused with 105 DFAT cells through the posterior orbital venous plexus once at 8 weeks of age. Mice were sacrificed at 12 weeks of age, and kidneys were removed. Protein samples were subjected to electrophoresis on polyacrylamide gels and then transblotted to nitrocellulose membranes. Blots were incubated with anti-TSG-6 polyclonal antibody and anti-TNF-α polyclonal antibody, and anti-beta actin antibody in TBST solution. Data are the mean ± SEM (n = 4). *P < 0.05 between with and without implantation of DFAT cells. DFAT dedifferentiated fat; SEM standard error of the mean; TNF, tumor necrosis factor; TSG-6 tumor necrosis factor-stimulated gene-6

Figure 9

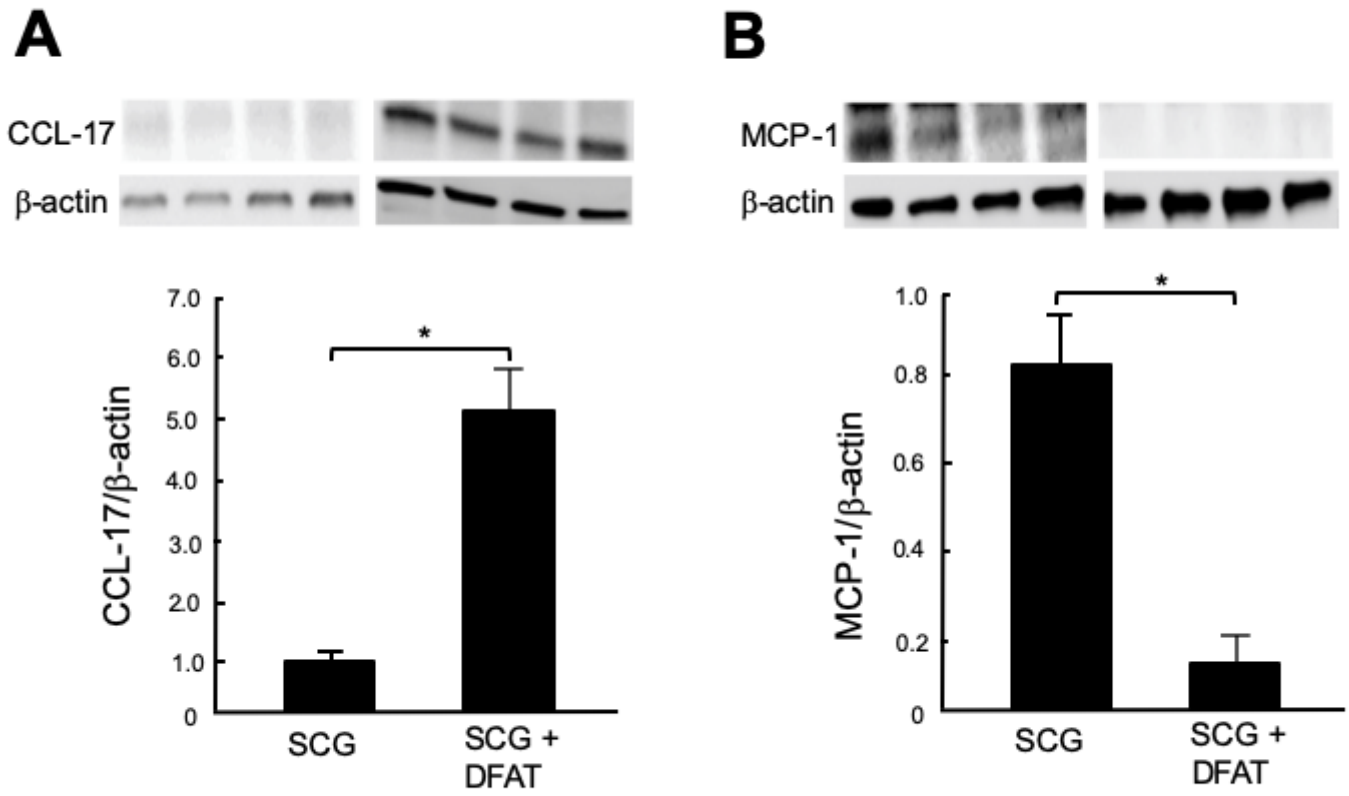

Figure 9

Effects of implantation of DFAT cells on expression of CCL-17 and MCP-1 proteins in kidney from SCG mice. SCG mice were infused with 105 DFAT cells through the posterior orbital venous plexus once at 8 weeks of age. Mice were sacrificed at 12-weeks of age, and kidneys were removed. Protein samples were subjected to electrophoresis on polyacrylamide gels and then transblotted to nitrocellulose membranes. Blots were incubated with anti-CCL-17 polyclonal antibody, anti-MCP-1 polyclonal antibody, and anti-beta actin antibody. Data are the mean ± SEM (n = 4). *P < 0.05. CCL-17 C-C Motif Chemokine Ligand 17; DFAT dedifferentiated fat; MCP-1 monocyte chemoattractant protein-1; SEM standard error of the mean

Figure 10

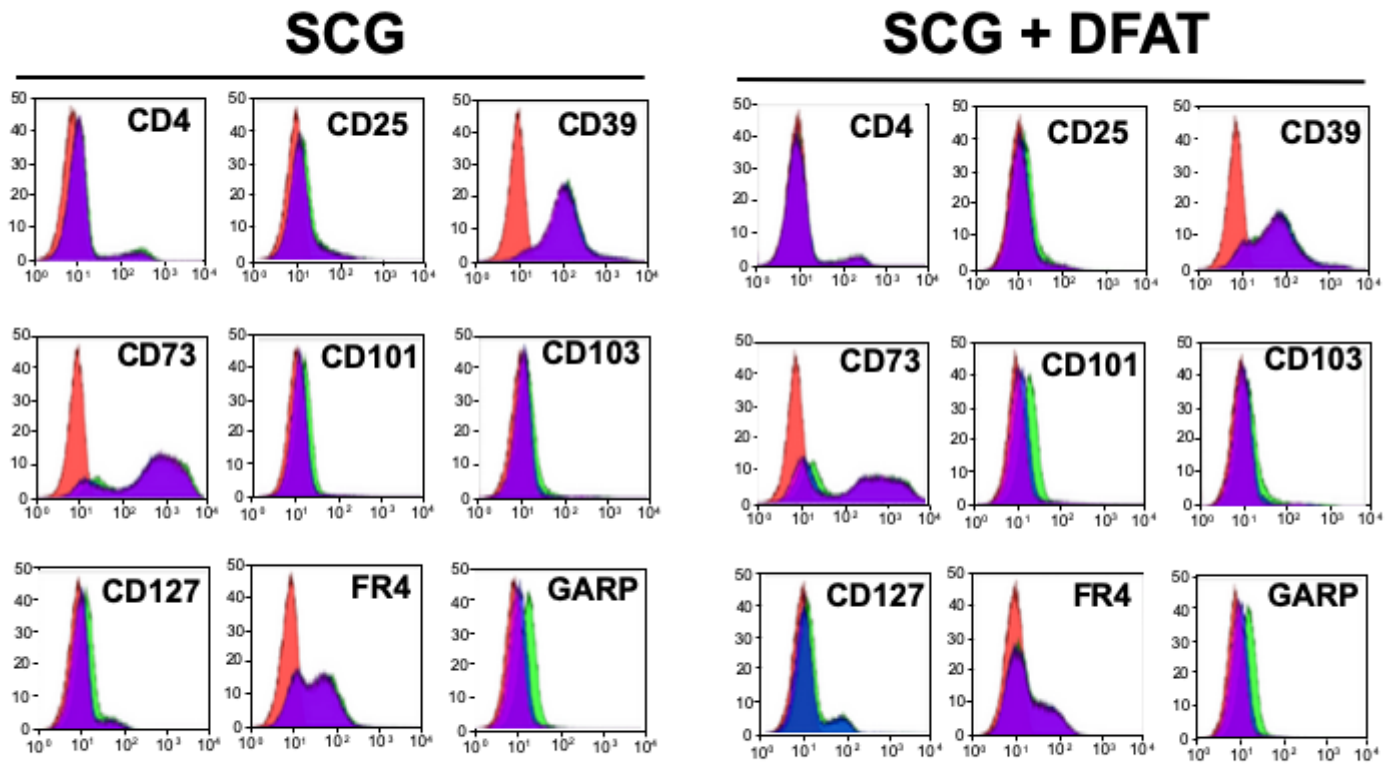

Figure 10

Effects of implantation of DFAT cells on the population of regulatory T cells in SCG mice. Spleen was removed and homogenized 4 weeks after implantation of 106 DFAT cells in SCG mice. Cells from spleen were labelled with fluorogenic antibodies to evaluate the proportion of CD4+ CD25+ FOXP3+ regulatory T cells. Cells were fixed and permeabilized with a FOXP3 Staining Buffer Set according to the manufacturer's instructions and included the blocking step with 2% rat serum. Flow cytometry was performed with a FACSAria system, and data were analyzed using FlowJo 7.6.5 software. DFAT dedifferentiated fat.

Supplementary Files

This is a list of supplementary files associated with this preprint. Click to download.

- 210924SUPPLEMENTARYMATERIALS.docx